Isolation Improvement Using Asymmetric Radiators and Ground Plane Diversity Mechanism in a Six-Element UWB MIMO Antenna Design

Aicha Mchbal[1, *], Naima Amar Touhami[1], Hanae Elftouh[1], and Aziz Dkiouak[2]

Abstract—A compact six elements MIMO antenna is presented for UWB applications. The proposed MIMO array consists of non-identical monopole antennas with distinctive ground planes so as to nullify mutual coupling amid side-by-side elements. Also, by properly placing the antenna elements exploiting cross polarization diversity, a good isolation throughout the operating bandwidth is achieved. Moreover, two parasitic inverted L stubs in combination with small rectangular stubs are employed near the middle-placed radiators and corner placed radiators, respectively, in order to extend the frequency band and enhance the impedance matching. Results show a good reflection coefficient about -10 dB, a high isolation > 20 dB, an envelope correlation coefficients < 0.15, a high diversity gain equal to 9.3, and finally, a maximum value of efficiency for both used antenna elements which is about 78% and 60% with 6 and 5 dBi of gain, respectively. They validate the proposed MIMO antenna efficiency for UWB diversity applications.

1. INTRODUCTION

Recently, high data rate and reliability are considered imperative for modern wireless communication systems, whereas ultra-wideband (UWB) technology remains an efficient solution to fulfill short range wireless systems for high throughput huge demand [1]. However, in spite of UWB technology ability of increasing data throughput as well as enhancing communication reliability, multipath fading is regarded as a big issue that alters this technology applications in modern wireless systems [2]. Thus, multiple-input multiple-output (MIMO) has been recognized for its capability to enhance signal quality as well as channel capacity without sacrificing additional transmitted power nor frequency spectrum [3]. A new concept that is based on incorporating UWB with MIMO systems so as to mitigate multipath fading and to boost data throughput has emerged [4].

The main purpose in MIMO systems is to establish parallel channels that intend to transmit and receive isolate signals, as well as increase channel capacity [5, 6]. Hence, the most challenging part while designing a MIMO system is to maintain a good isolation amid antenna elements through minimizing their electromagnetic coupling [7, 8]. Many reported works have addressed this challenge by using different techniques including: metamaterial isolator, decoupling structure, parasitic isolator, patterned grounds, meander line resonator, frequency selective surface (FSS), defected ground structure (DGS), neutralization lines/etching slots on the ground plane, using electromagnetic band gap (EBG) structures, deploying decoupling or matching networks, introducing parasitic structures, properly placing the antenna elements, changing radiation patterns, and introducing neutralization line [2, 9]. However, most of these researches are for $2 * 2$ or $4 * 4$ MIMO antenna configuration, ignoring contemporary

* Corresponding author: Aicha Mchbal (aicha.mchbal8@gmail.com).
[1] Faculty of Sciences, Abdelmalek Essaadi University, Tetuan, Morocco. [2] National School of Applied Sciences, Abdelmalek Essaadi University, Tetuan, Morocco.

wireless communication systems needs of high channel capacity which implies their needs for high order MIMO antenna design [10, 11].

In this paper, a novel six-port MIMO antenna for UWB applications is investigated. The presented MIMO antenna exploits distinct mechanisms for inter-element electromagnetic coupling reduction. Basically, without involving any decoupling structure and by employing spatial and cross polarization diversity, a minimum level of mutual coupling is achieved. The mutual coupling reduction is based on using different shapes of monopole antenna elements with different ground planes so as to achieve pattern diversity. A wide bandwidth is obtained by introducing parasitic stubs on the top side of the used substrate as well as by defecting antenna elements feedlines. The measured MIMO performances such as envelope correlation coefficient, diversity gain, efficiency, gain, and far-field characteristics prove that the studied MIMO antenna is useful for diversity applications where pattern diversity is a figure of merit.

This paper is organized as follows. In Section 2, a full description of antenna design evolution is discussed. Section 3 is dedicated to MIMO antenna fabrication process and measurements, while the antenna diversity performance evaluation is presented in Section 4. Finally, the manuscript is concluded in Section 5.

2. PROPOSED ANTENNA DESIGN PROCESS

2.1. Single Antenna Configuration

A full description of the adopted single-element owl-shaped antenna design process is discussed in this section. The adopted antenna is mounted on the top face of a low cost $26*15.5*0.8\,\text{mm}^3$ FR-4 substrate with a relative permittivity 4.3 and loss tangent 0.025. Note that the adopted antenna has evolved from an owl-shaped $2*2$ MIMO antenna in [12], and it is simulated in the well-known 3-D electromagnetic simulator CST MWS. Table 1 illustrates the optimized dimensions of the proposed owl-shaped single antenna element.

Table 1. The optimized dimensions of the adopted single antenna in (mm).

Parameter	Value	Parameter	Value
L	31	W	15
L_1	8.3	W_1	10
L_2	8	W_2	11
L_f	9	W_f	1
L_{s1}	4	W_{s1}	0.8
L_{s2}	1	W_{s2}	1
J	6	S	0.5
R	2.5	R_1	5

Basically, the antenna element has evolved from a simple rectangular patch antenna. With the aim of covering a wide bandwidth, a partial ground plane with different defects has been employed. An arc-shaped structure and a semi-circle with an open-ended slot are introduced on the patch, in order to extend the operating frequency band and to shift the lower frequency. Furthermore, defecting has been done on the ground plane so as to enhance the impedance matching and isolation simultaneously. Figure 1 depicts the adopted single element antenna.

2.2. $2*2$ MIMO Antenna Assembly

A profound study of a $2*2$ MIMO antenna with two configurations is accomplished in this section. This investigation is based on mutual coupling comparison between two different designs taking into account the antenna elements arrangement. Note that the first design consists of two face-to-face placed
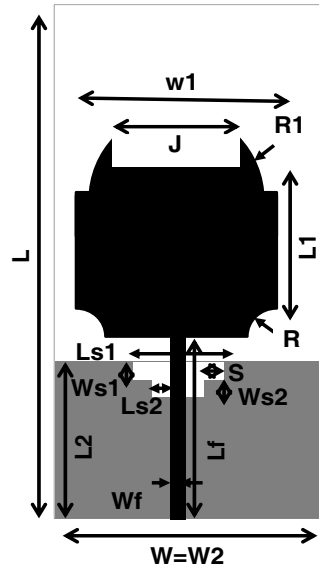
Figure 1. The adopted single patch antenna.
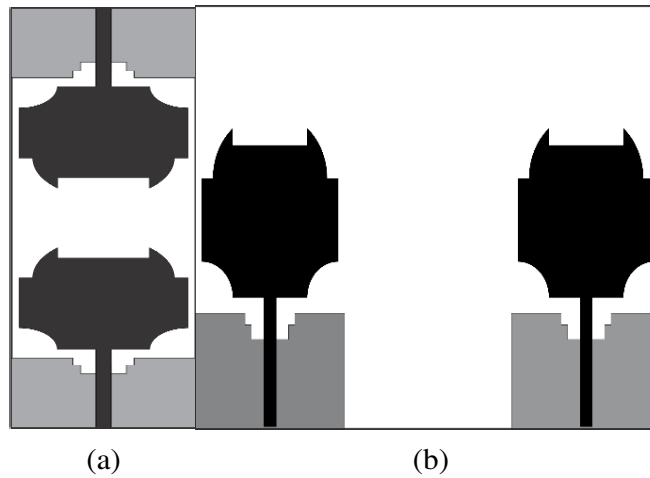
Figure 2. The proposed MIMO antenna designs, (a) first design, (b) second design.

radiators, and the second configuration is composed of two side-by-side placed MIMO antenna elements in which the antenna elements arrangement is based on spatial diversity technique. Figures 2(a) and (b) illustrate the $2 * 2$ MIMO antenna configurations.

As depicted in Figure 3 that represents the comparison of the simulated impedance matching and the electromagnetic coupling of the two configurations, simulated results show that configuration 1 exhibits low mutual coupling compared with configuration 2, which prove the efficiency of configuration 1 and utility at its incorporating level on high order MIMO antenna.

2.3. $4 * 4$ MIMO Antenna Array

Based on the studied $2*2$ MIMO array results, a $4*4$ MIMO antenna design is carried out. The proposed antenna configuration is based on spatial diversity and cross polarization diversity employment since it has been shown the efficiency of both configurations. Figure 4 exhibits the proposed $4 * 4$ MIMO antenna array.

The simulated reflection coefficient as well as mutual coupling of the investigated $4*4$ MIMO array
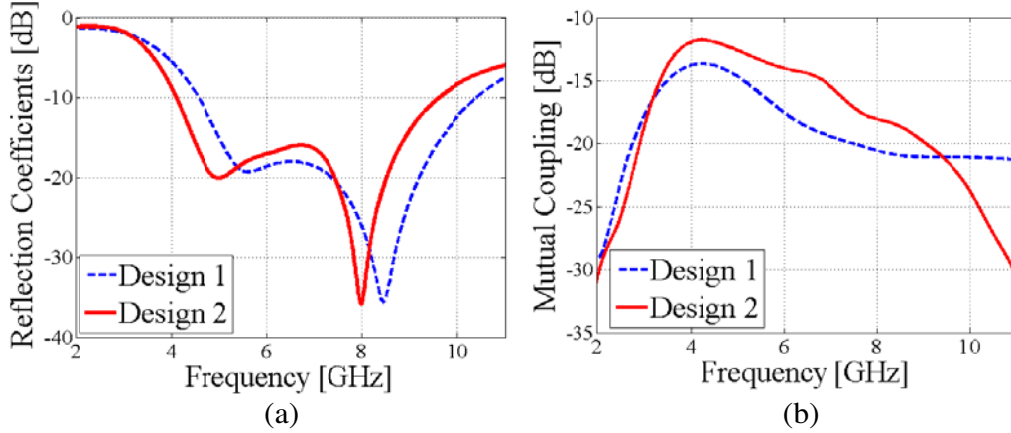
Figure 3. The scattering parameters of the proposed configurations, (a) return loss, (b) electromagnetic coupling.
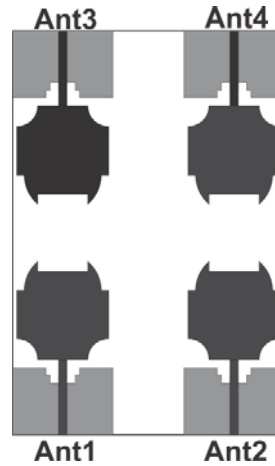
Figure 4. The presented four-element MIMO antenna design.

is presented in Figure 5. As shown, a good impedance matching about -20 dB is achieved, and high isolations about -10, -12, and -23 dB are obtained over the operation frequency band, which prove the configuration efficiency of studied MIMO antenna on maintaining a low electromagnetic coupling between adjacent elements.

2.4. $6 * 6$ MIMO Antenna System

The previous $4 * 4$ MIMO antenna results motivate us to elaborate a high order MIMO antenna that consists of six elements, so in the same way, the studied owl-shaped single antenna is adopted in this $6 * 6$ MIMO antenna configuration. Also, an optimized location of antenna elements is used. Simulation study of the presented design has been performed using the well-known CST Microwave Studio (MWS) simulator. Figures 6(a), (b), (c), (d), and (e) represent the proposed $6 * 6$ MIMO antenna design evolution.

The main objective of the first design step is to arrange the radiators properly in such a way that we can ensure an acceptable port-to port mutual coupling as well as a compact size. Figures 7(a) and (b) represent the scattering S-parameters of the first antenna design. Note that due to symmetry, only S_{11}, S_{22}, S_{12}, S_{14}, S_{15}, S_{23}, S_{24}, S_{26} have been represented.

It is noticeable that thanks to cross ((Ant2, Ant5), (Ant2, Ant6), (Ant1, Ant4), (Ant1, Ant6), (Ant3, Ant4), and (Ant3, Ant5)), face-to-face ((Ant2, Ant4), (Ant1, Ant5), (Ant3, Ant6)), and side-by-
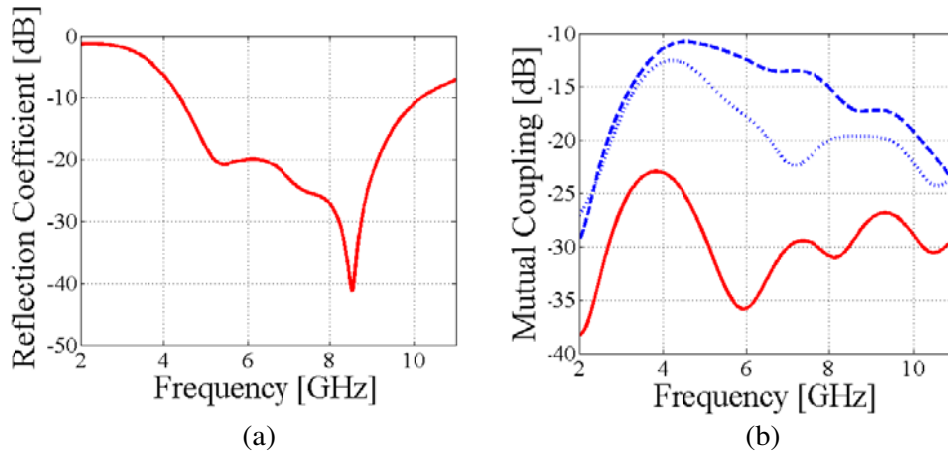
Figure 5. S-parameters of the studied $4*4$ MIMO antenna array, (a) reflection coefficient, (b) mutual coupling.

side ((Ant1, Ant2), (Ant1, Ant3), (Ant2, Ant3), (Ant6, Ant5), (Ant6, Ant4), (Ant5, Ant4)) antenna arrangement, good isolations about 25, 14, and 15 dB are achieved, respectively. However, a high mutual coupling between small spaced antenna elements ((Ant1, Ant2), (Ant1, Ant3), (Ant4, Ant5)), (Ant5, Ant6)) is declenched which is about -8.16 dB throughout [3.86–5.09] GHz, and a bad impedance matching over the UWB operating frequency band has been shown.

To deal with the impedance matching enhancement in order to cover the UWB of interest as well as to get the antenna prepared to the employment of pattern diversity, a modification at ground plane level has been done. Figures 7(c) and (d) illustrate the return loss and the electromagnetic mutual coupling of the proposed antenna design second step. As depicted, a slight improvement at S_{12} and S_{11} has been realized.

So, in order to improve the isolation between really closed radiators [S_{12}, S_{13}, S_{45}, S_{56}], a novel approach is based on the deployment of different antenna elements so as to purchase pattern diversity antenna that can be employed in diversity applications. Figures 7(e), (f) show the impedance matching as well as the isolation of the third step of presented antenna configuration. It is obvious that after performing a parametric study on the radiators, the isolation is improved from -8.16 to -11 dB over [2.8–3.64] GHz with always a bad impedance matching and a narrow bandwidth.

As a solution to this issue, a defected microstrip structure has been employed on the feedlines, to enhance the impedance matching and extend the operating frequency band in order to cover the UWB bandwidth. Figures 7(g), (h) exhibit the reflection coefficients and the mutual coupling of the fourth step of antenna design. It is clear that S_{11} is improved to purchase -15 dB throughout [4.64–13] GHz and $S_{22} < -10$ dB from 2.96 to 10.69 GHz. However, S_{24} tends to be -8 dB across [2.47–3.68] GHz frequency band.

Finally, in order to improve the adaptation more and cover the desired UWB frequency, a pair of inverted L parasitic stubs has been introduced on the top side of the used substrate near the feedline of each middle-placed antenna element. Also, small rectangular stubs have been employed on the top side corners of the substrate, noting that these later intend to absorb the coupling between elements as well as to shift the lower frequency. Figures 7(i) and (j) display S-parameters of the last antenna design. As revealed, a good isolation is achieved between cross-polarized, face-to-face, and parallel antenna elements about ($S_{14} < -24$, $S_{26} < -18$), 12, and ($S_{24} < -10$ and $S_{15} < -20$) dB, respectively. Also, a UWB has been covered that ranges from 3.1 to 13 and 1 to 10.6 GHz for S_{11} and S_{22}, respectively. With about -13 dB impedance matching. Figures 8(a), (b) manifest the layout of proposed six-element UWB MIMO antenna, and its optimized dimensions are displayed in Table 2.

2.5. Current Distribution

The vector current distribution analysis of the designed MIMO antenna is considered really helpful to represent the radiating behavior of a certain antenna element. Figures 9(a), (b), (c), and (d) illustrate

the current distribution of antenna when port 1 and port 2 are excited at 3.5 GHz while others are terminated to 50 Ω matched impedance with and without the used decoupling mechanism.

As shown, it is clear that the presented MIMO antenna exhibits low port-to-port electromagnetic coupling after the employment of the proposed mutual decoupling approach, which has already been
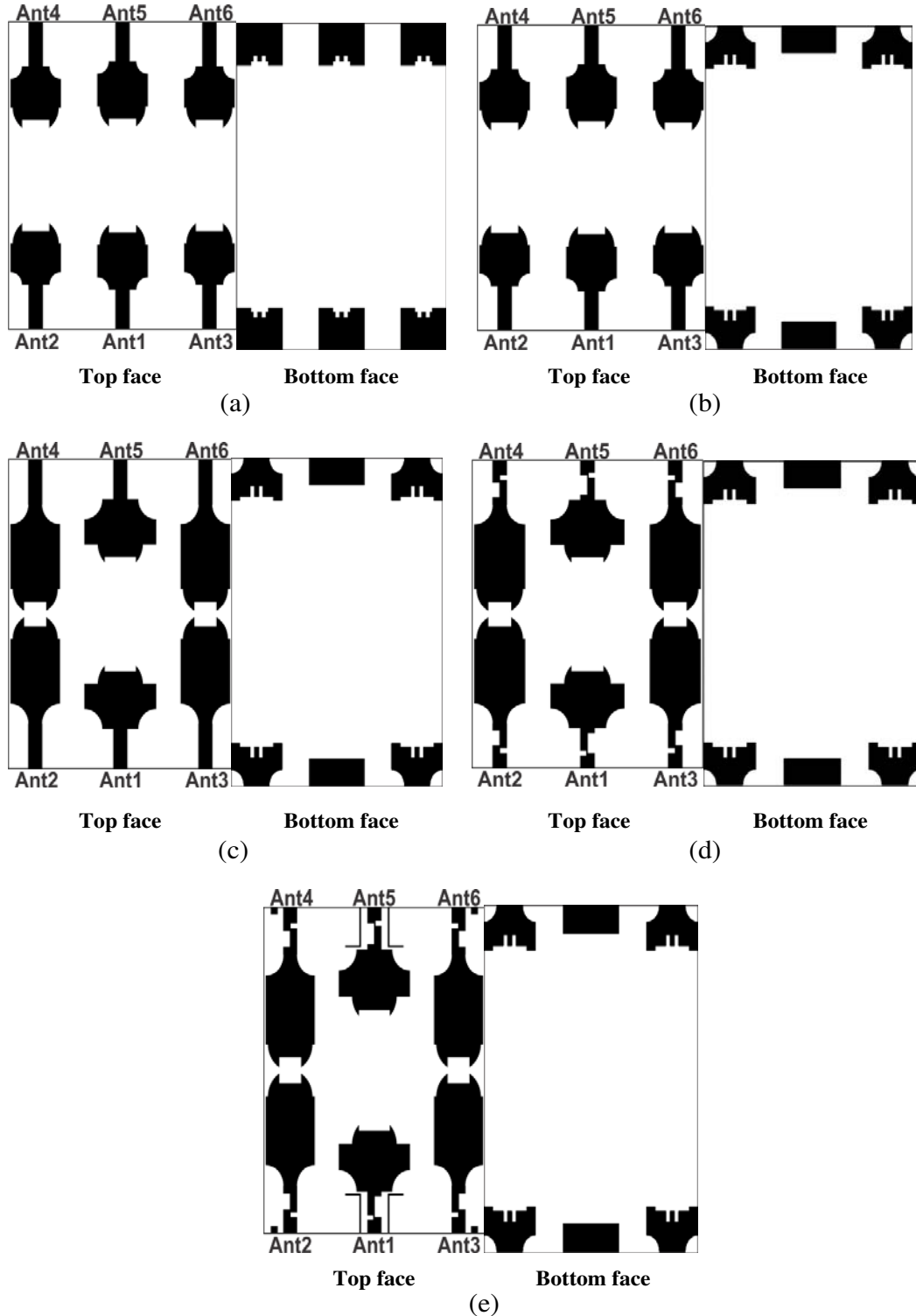
Figure 6. The proposed six-element MIMO antenna design evolution, (a) first step design, (b) second step design, and (c) third step design, (d) fourth step design, (e) fifth step design.

manifested in mutual coupling characteristic curve presented in Figure 7(h), which proves that the peculiar arrangement in combination with ground plane and radiators diversity are responsible for the suppression of the coupled currents amid radiators that are caused by coupled fields.

2.6. Efficiency and Gain

The parameters that contribute to revealing the presented MIMO antenna assembly performance are radiation efficiency and antenna gain. Figure 10 depicts the radiation efficiency and gain of both antenna elements. As depicted, a reasonable efficiency of maximum values about 78% and 60% that correspond respectively to port 2 and port 1 has been obtained in covered [3.1–10.6] frequency band, which makes
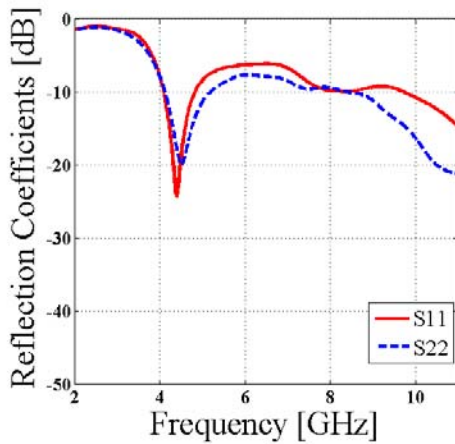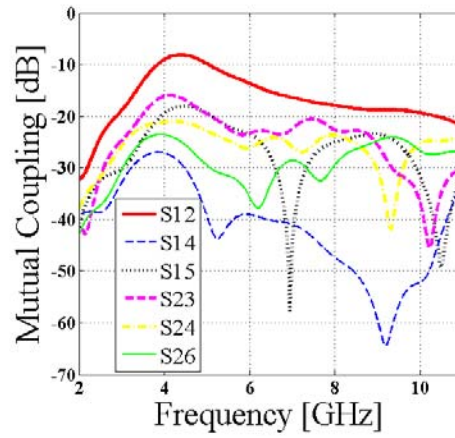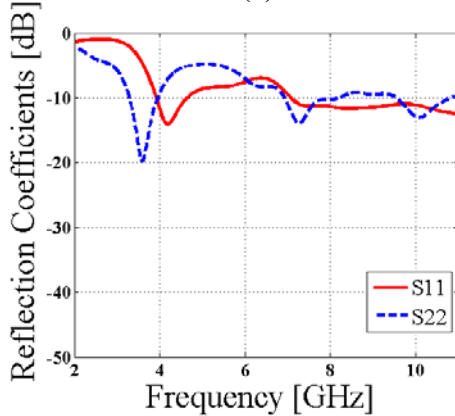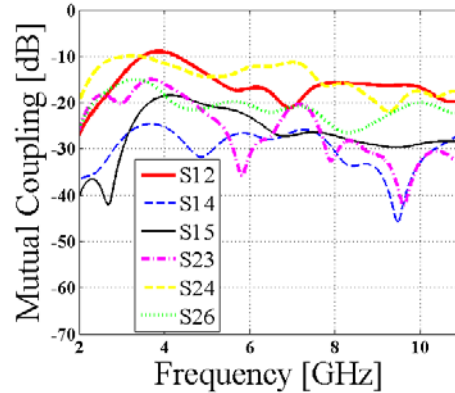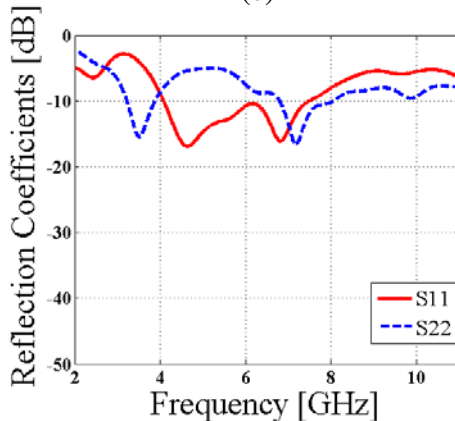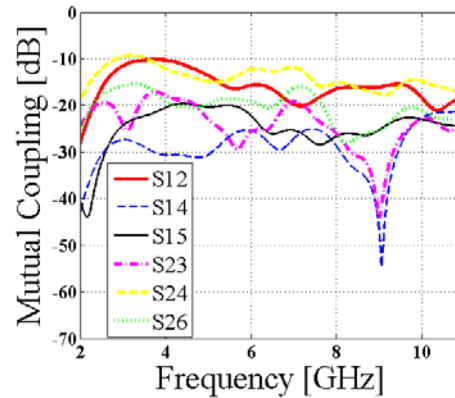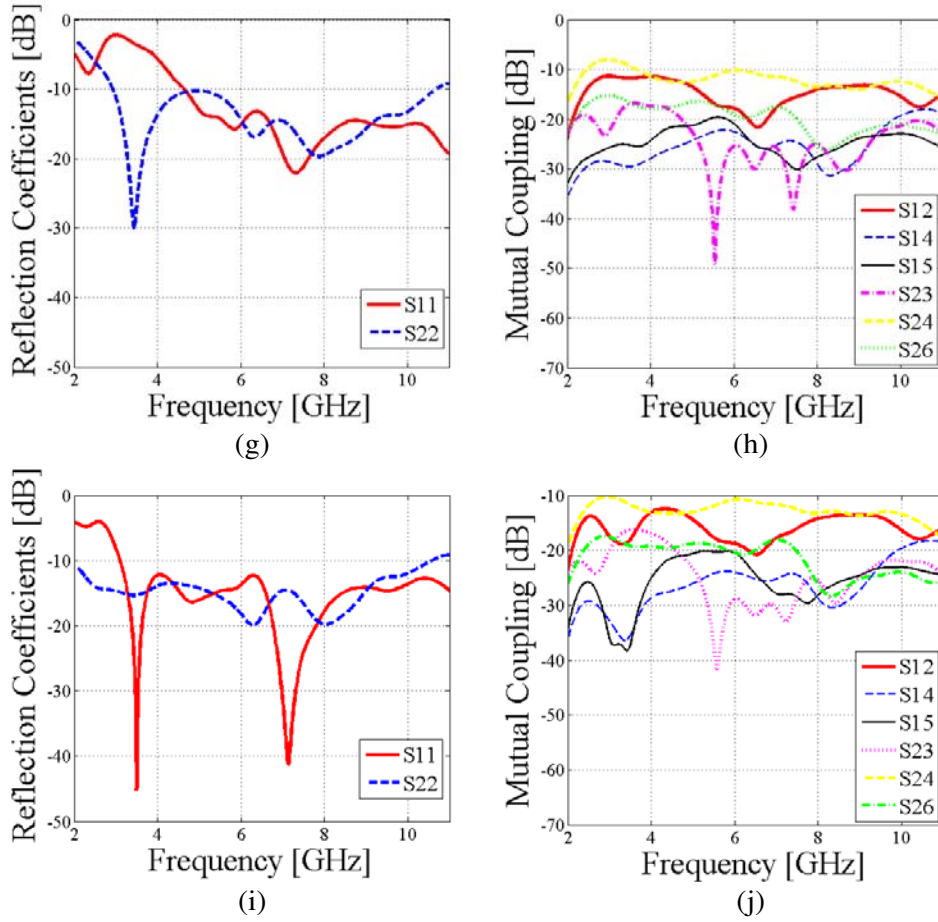
Figure 7. Simulated S-parameters of the investigated MIMO antenna, (a), (b) first step; (c), (d) second step; (e), (f) third step; (g), (h) fourth step; (i), (j) final step.
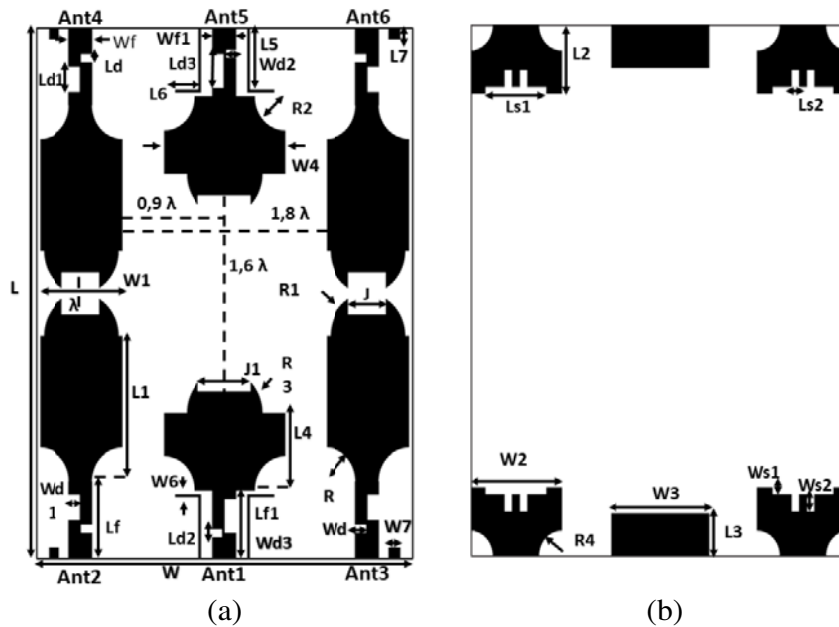
Figure 8. The proposed six-element MIMO antenna final design, (a) top face, (b) bottom face.

Table 2. The optimized dimensions of the studied six elements UWB MIMO antenna in (mm).

Parameter	Value	Parameter	Value
L	62	W	50
L_1	17	W_1	11
L_2	8	W_2	12
L_3	5	W_3	13
L_4	9	W_4	16
L_5	7.5	W_5	0.3
L_6	3.2	W_6	0.3
L_7	1.5	W_7	1.3
L_f	9	W_f	3.1
L_{f1}	8	W_{f1}	3.1
L_d	1	W_d	1.5
L_{d1}	3	W_{d1}	1.5
L_{d2}	1	W_{d2}	1.3
L_{d3}	4	W_{d3}	1.5
L_{s1}	8	W_{s1}	0.8
L_{s2}	1	W_{s2}	2
R	4	R_1	5
R_2	4	R_3	5
R_4	3	S	1
J	5	J_1	7
T	0.035	H	1.6

the antenna array an efficient radiation system. Also, despite defects on the ground plane and its effect on the antenna gain, results show that adding some parasitic stubs on the substrate top side could compensate the gain degradation. Thus, the highest gain values about 6 and 5 dBi have been achieved.

3. FABRICATION PROCESS

The printed circuit board technology has been used to fabricate the model of the presented six-element MIMO antenna. Rohde and Schwarz ZVB 20 vector network analyser has been utilized in the scattering parameters measurement in such a way that two antenna elements are connected to it, while the rest of radiators are terminated by 50 Ω loaded impedance. Figure 11 presents photographs of the fabricated MIMO antenna.

As observed in Figures 12 and 13 that exhibit measured S-parameters, there is a fair agreement between simulated and measured results, noting that some discrepancies can be seen between measured and simulated results, which are attributed to the used SMA connectors tolerance, termination resistance, fabrication inaccuracy, and soldering. So, measured results show a good impedance matching about −10 dB over the desired frequency band and a high isolation about 20 dB.

4. ANTENNA DIVERSITY PERFORMANCE

The evaluation of MIMO antennas diversity performance can be verified through certain metrics measurement, such as envelope correlation coefficient (ECC), diversity gain (DG), Total Active Reflexion Coefficient (TARC), and channel capacity (CLL), without forgetting characteristic far field for sure. Note that ECC and CLL thresholds are defined at 0.5, while TARC should be < 0 dB.
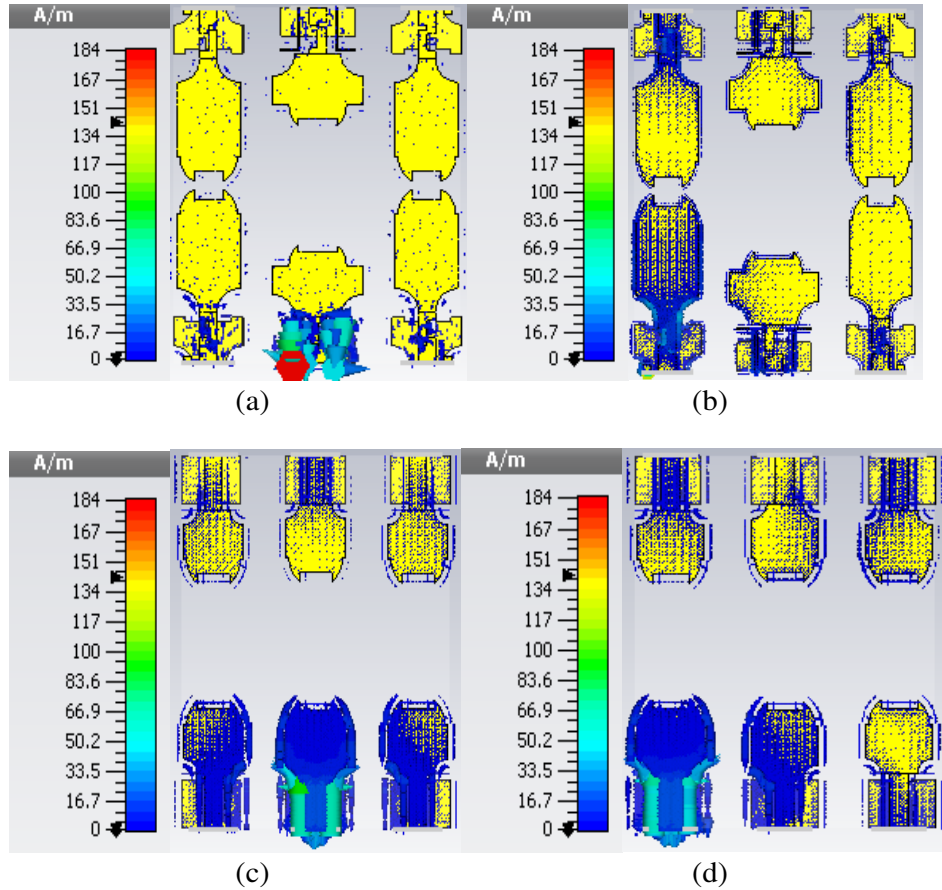
Figure 9. Current distribution comparison of the proposed MIMO antenna at 3.5 GHz with and without the decoupling mechanism; (a) and (b) when Ant1 and Ant2 are excited, respectively with the used decoupling mechanism, (c) and (d) when Ant1 and Ant2 are 7 excited without the used decoupling mechanism.
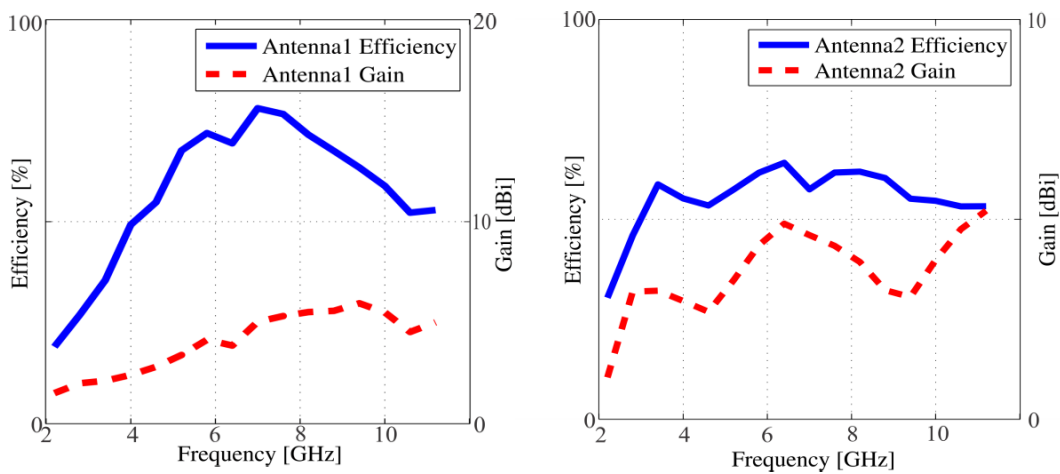
Figure 10. Simulated gain and efficiency of the presented MIMO antenna.

4.1. Envelope Correlation Coefficient

Envelope correlation coefficient is regarded as a critical parameter on MIMO antenna performance analysis, and it describes how much decorrelated the radiation patterns are at information reception
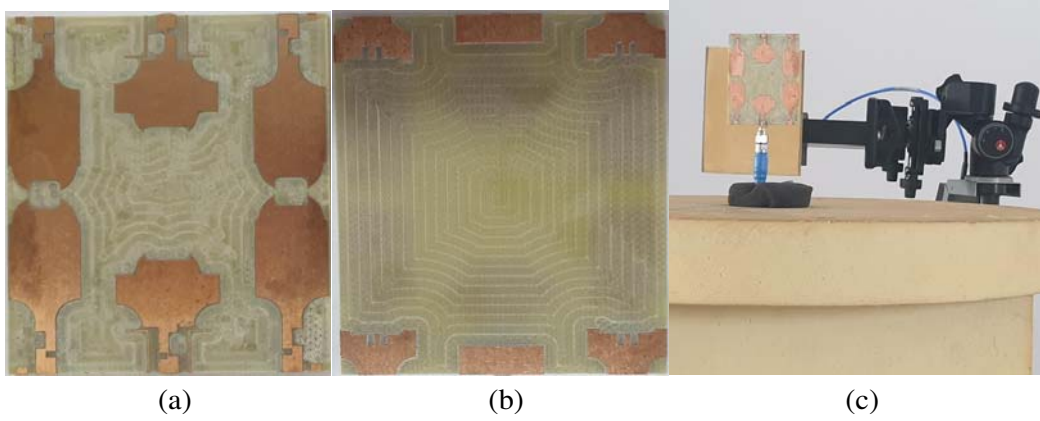
Figure 11. Photographs of the presented MIMO antenna, (a) top side, (b) bottom side, (c) pattern measurement.
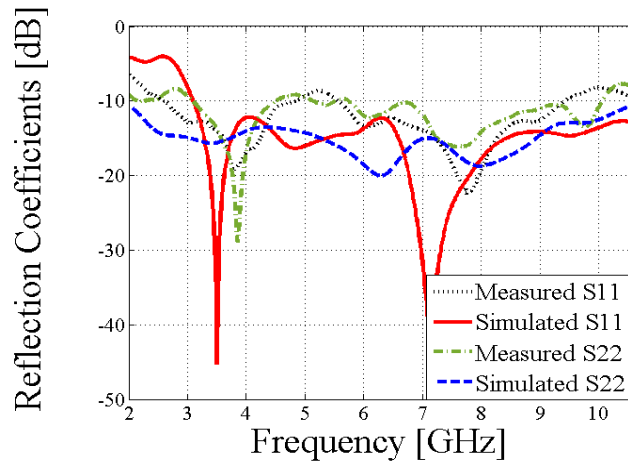
Figure 12. Simulated and measured return loss comparison.

level. In general, there are two different methods for ECC calculation, S-parameters and far-field based methods [13]. Note that the calculation of ECC using the scattering parameters is only valid for lossless antennas, while the 3 D radiation pattern based ECC that is expressed by Equation (1) is dedicated for lossy antennas [14]. Figure 14 represents the simulated and measured far-field envelope correlation coefficients.

$$\rho\left(i,j\right) = \frac{\left|\iint_{4\pi}\left[F_i\left(\theta,\O\right) * F_j\left(\theta,\O\right)\right]d\Omega\right|^2}{\iint_{4\pi}\left|F_i\left(\theta,\O\right)\right|^2 d\Omega * \iint_{4\pi}\left|F_j\left(\theta,\O\right)\right|^2 d\Omega} \tag{1}$$

where $F_i(\theta,\Phi)$ is the farfield pattern of the ith antenna.

The diversity gain (DG) of the studied MIMO antenna is related to the calculated ECC value as shown in Equation (2) [15]. Figure 15 displays the investigated MIMO antenna diversity gain.

$$\mathrm{DG} = 10\sqrt{1 - \left|\rho_{i,j}\right|^2} \tag{2}$$

To predict the performance of a MIMO antenna system, a conventional scattering matrix is considered not sufficient enough. Total Active Reflection Coefficient has been proposed. This metric gives an idea concerning the overall match of the MIMO system taking into consideration the electromagnetic

coupling effects between ports [16]. Formula (3) can be used for MIMO TARC calculation.

$$\Gamma = \frac{\sqrt{\sum_{i=1}^{N} |b_i|^2}}{\sqrt{\sum_{i=1}^{N} |a_i|^2}} \tag{3}$$

where a_i and b_i indicate the incident and reflected signals, respectively.

$$[b] = [S][a] \tag{4}$$

According to six-element MIMO antenna system, Equation (5) could be written as follows:

$$\begin{bmatrix} b1 \\ b2 \\ b3 \\ b4 \\ b5 \\ b6 \end{bmatrix} = \begin{bmatrix} S11 & S12 & S13 & S14 & S15 & S16 \\ S21 & S22 & S23 & S24 & S25 & S26 \\ S31 & S32 & S33 & S34 & S35 & S36 \\ S41 & S42 & S43 & S44 & S45 & S46 \\ ?51 & S52 & S53 & S54 & S55 & S56 \\ S61 & S62 & S63 & S64 & S65 & S66 \end{bmatrix} \begin{bmatrix} a1 \\ a2 \\ a3 \\ a4 \\ a5 \\ a6 \end{bmatrix} \tag{5}$$

Figure 16 illustrates the TARC of the proposed MIMO antenna while considering port 1 is the first excited port ($\Theta1 = 0$), and the other ports are excited with following phases: $\Theta2 = 40$, $\Theta3 = 60$, $\Theta4 = 80$, $\Theta5 = 90$, $\Theta6 = 120$, $\Theta7 = 180$, $\Theta8 = 240$.

(a)

(b)

(c)

(d)
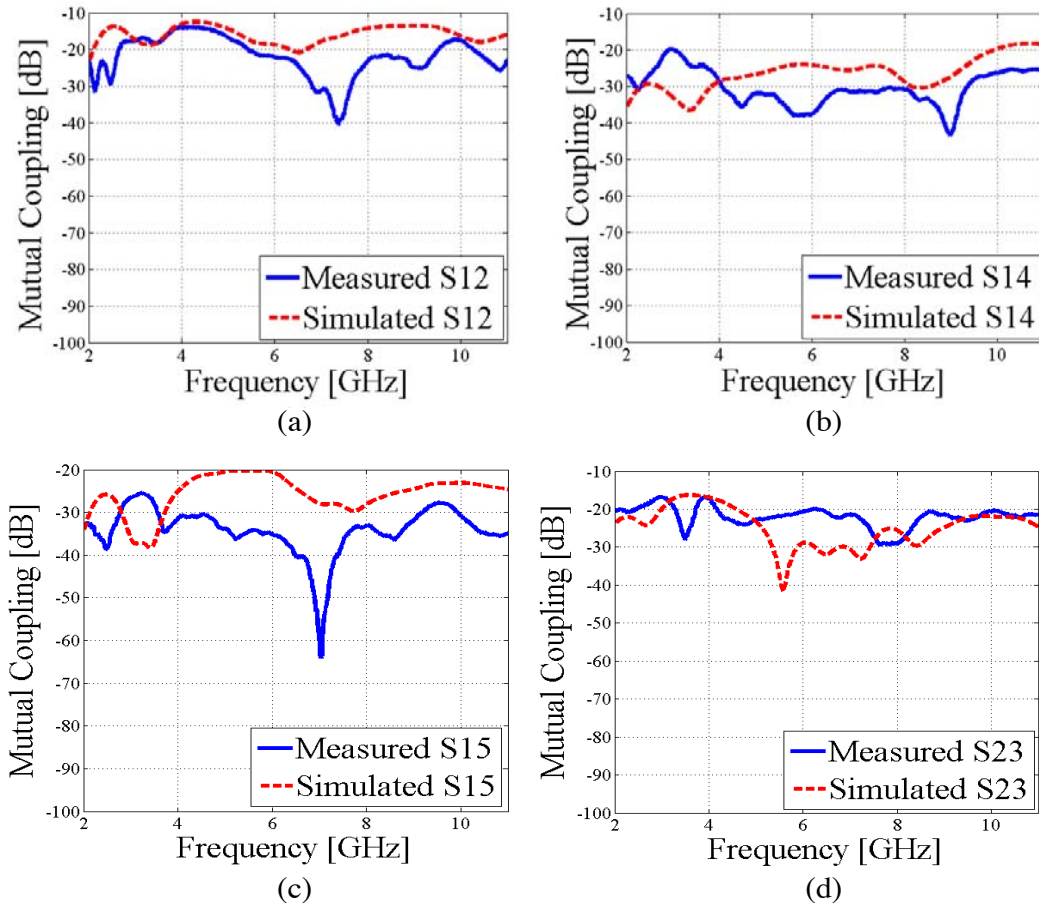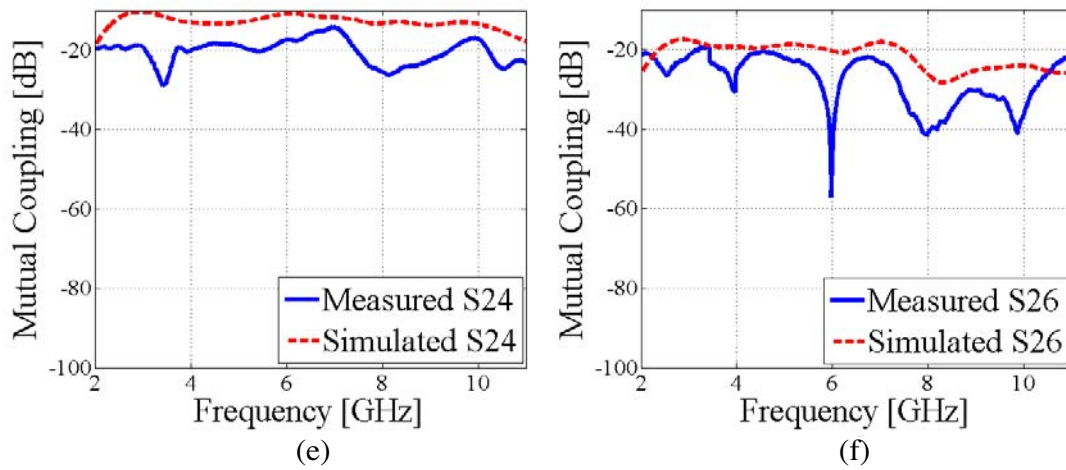
Figure 13. Simulated and measured coupling comparison, (a) simulated and measured S_{12}, (b) simulated and measured S_{14}, (c) simulated and measured S_{15}, (d) simulated and measured S_{23}, (e) simulated and measured S_{24}, (f) simulated and measured S_{26}.

(e)   (f)
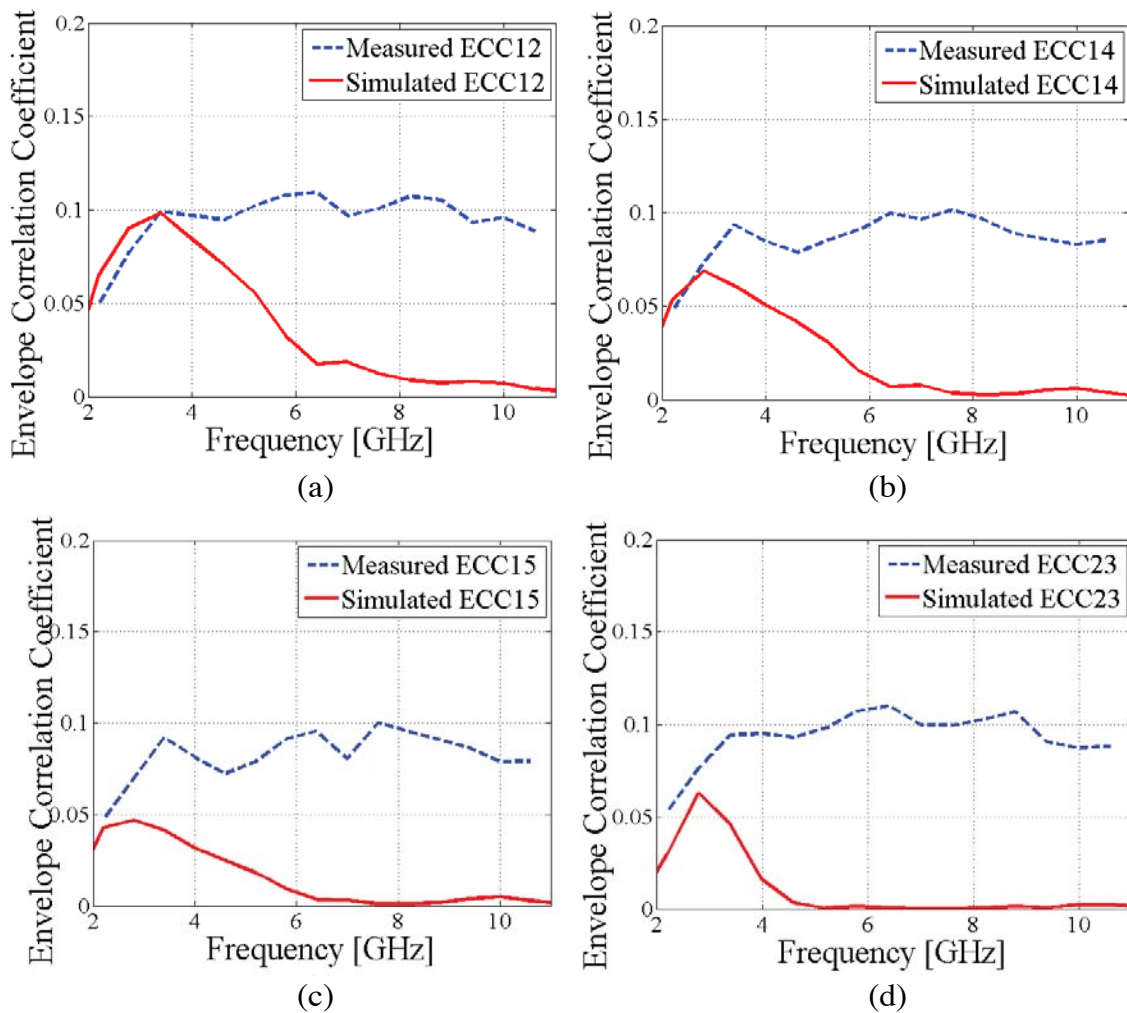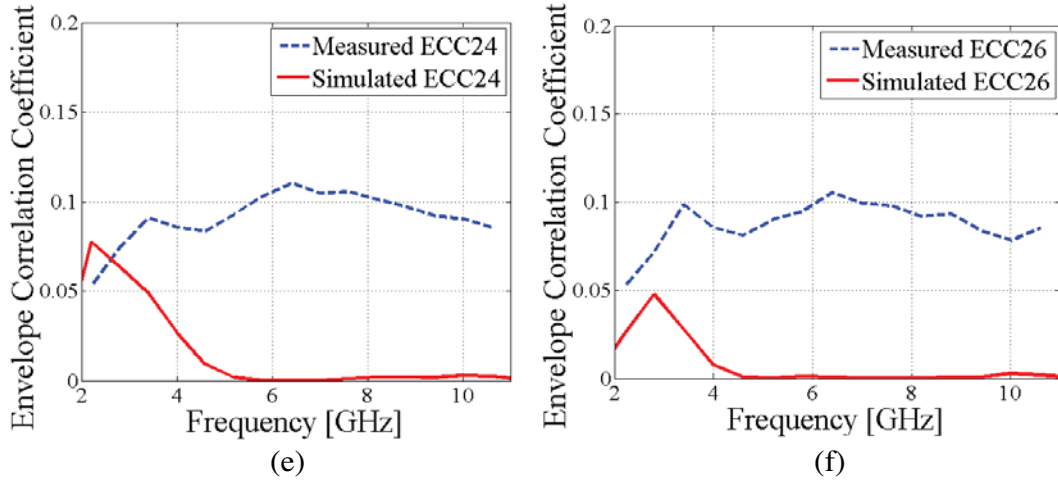
Figure 14. Simulated and measured envelope correlation coefficients comparison, (a) simulated and measured ECC12, (b) simulated and measured ECC14, (c) simulated and measured ECC15, (d) simulated and measured ECC23, (e) simulated and measured ECC24, (f) simulated and measured ECC26.

4.2. Radiation Characteristics

The radiation characteristics of the studied MIMO antenna are also presented. Figures 17 and 18 illustrate the simulated and measured normalized E-field and H-field comparison at 3.5, 7.14, and 9.5 GHz for antenna 1 and antenna 2, respectively, when one antenna is excited while others are terminated to a 50 Ω matching load. As illustrated, both antenna elements exhibit a quasi-omnidirectional behavior. Note that because of measurements constraints and lack of anechoic chamber, a slight difference between simulated and measured patterns has been observed.

5. PERFORMANCE COMPARISON

To validate the proposed MIMO antenna performance, a comparison between this and other reported MIMO systems should be taken into consideration. Table 3 presents a comparison in terms of dimensions, number of antenna elements, bandwidth, isolation, and envelope correlation coefficient. As depicted in Table 3, the presented MIMO assembly shows a small size, wide bandwidth, high isolation, and low mutual coupling compared with the cited works, which proves the efficiency of investigated antenna.

Table 3. Antenna performance comparison.

Ref.	Dimensions (mm)	Bandwidth (GHz)	Isolation (dB)	ECC	No. of Ants
This work	62 ∗ 50	3.1–10.6	> 20	< 0.15	6
[17]	120 ∗ 70	2.55–2.60 3.51–3.65	> 20	< 0.5	6
[18]	150 ∗ 150	1.55–3.8 5.6–6	> 10	< 0.1	6
[19]	136 ∗ 68.8	1.8–1.92 2.3–2.62	> 10	< 0.16	6
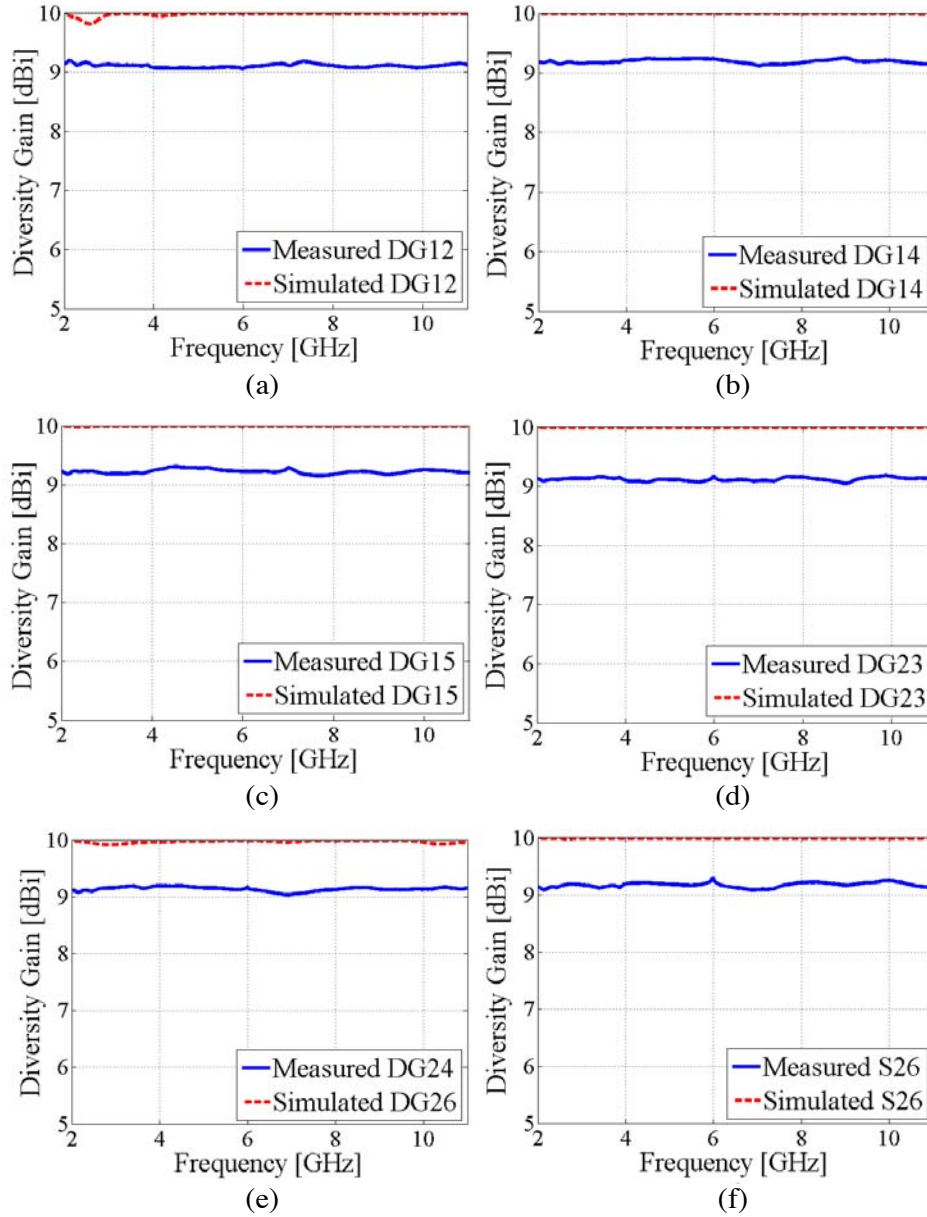
Figure 15. Simulated and measured diversity gain comparison, (a) simulated and measured DG12, (b) simulated and measured DG14, (c) simulated and measured DG15, (d) simulated and measured DG23, (e) simulated and measured DG24, (f) simulated and measured DG26.
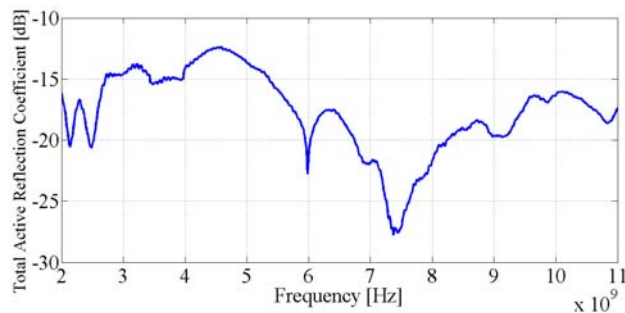
Figure 16. Measured total active reflexion coefficient.
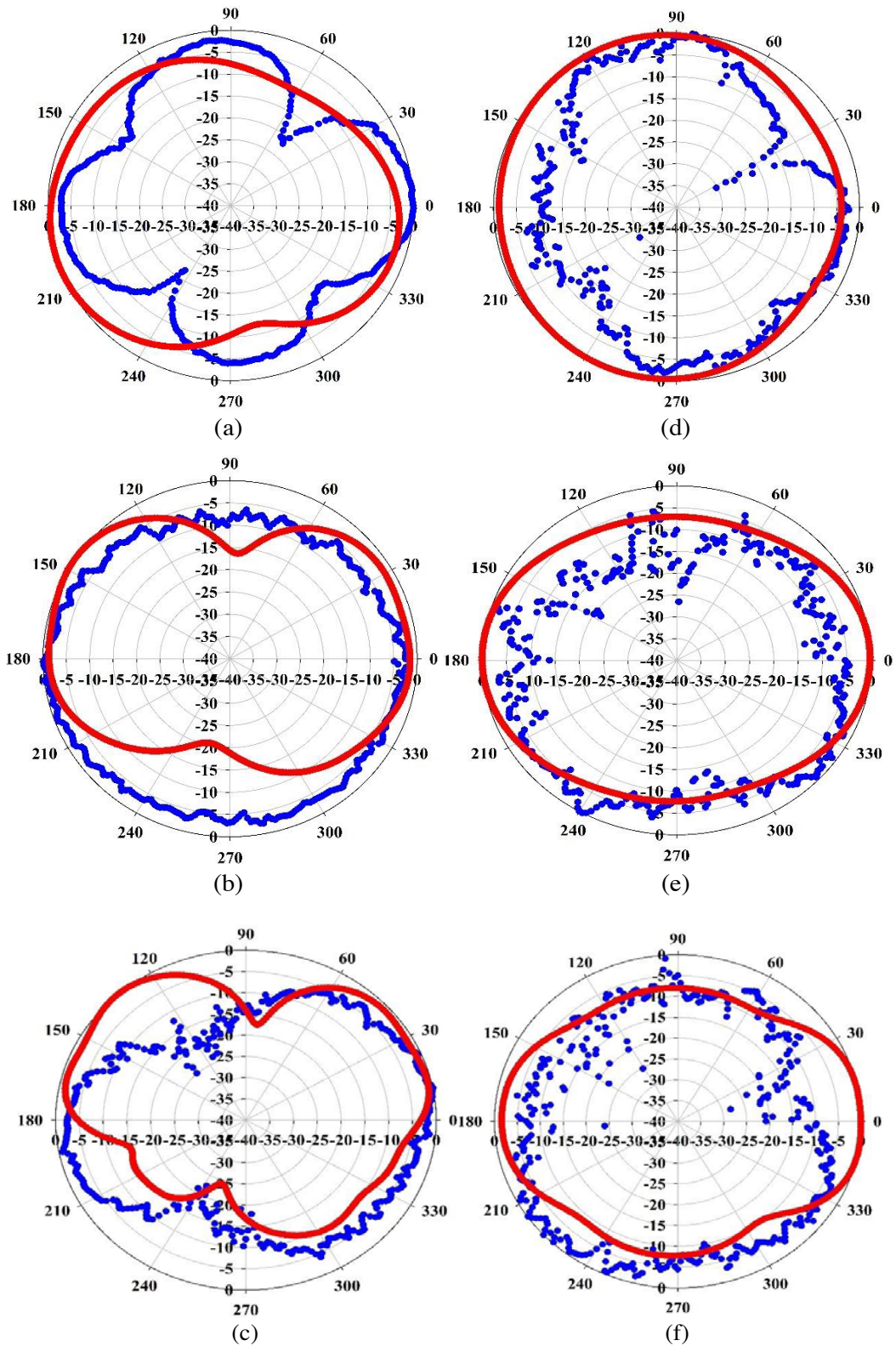
Figure 17. Simulated and measured radiation patterns of antenna 1 at 3.5 GHz, 7.14 GHz, and 9.5 GHz, (a), (b), (c) *E*-plane, and (d), (e), (f) *H*-plane.
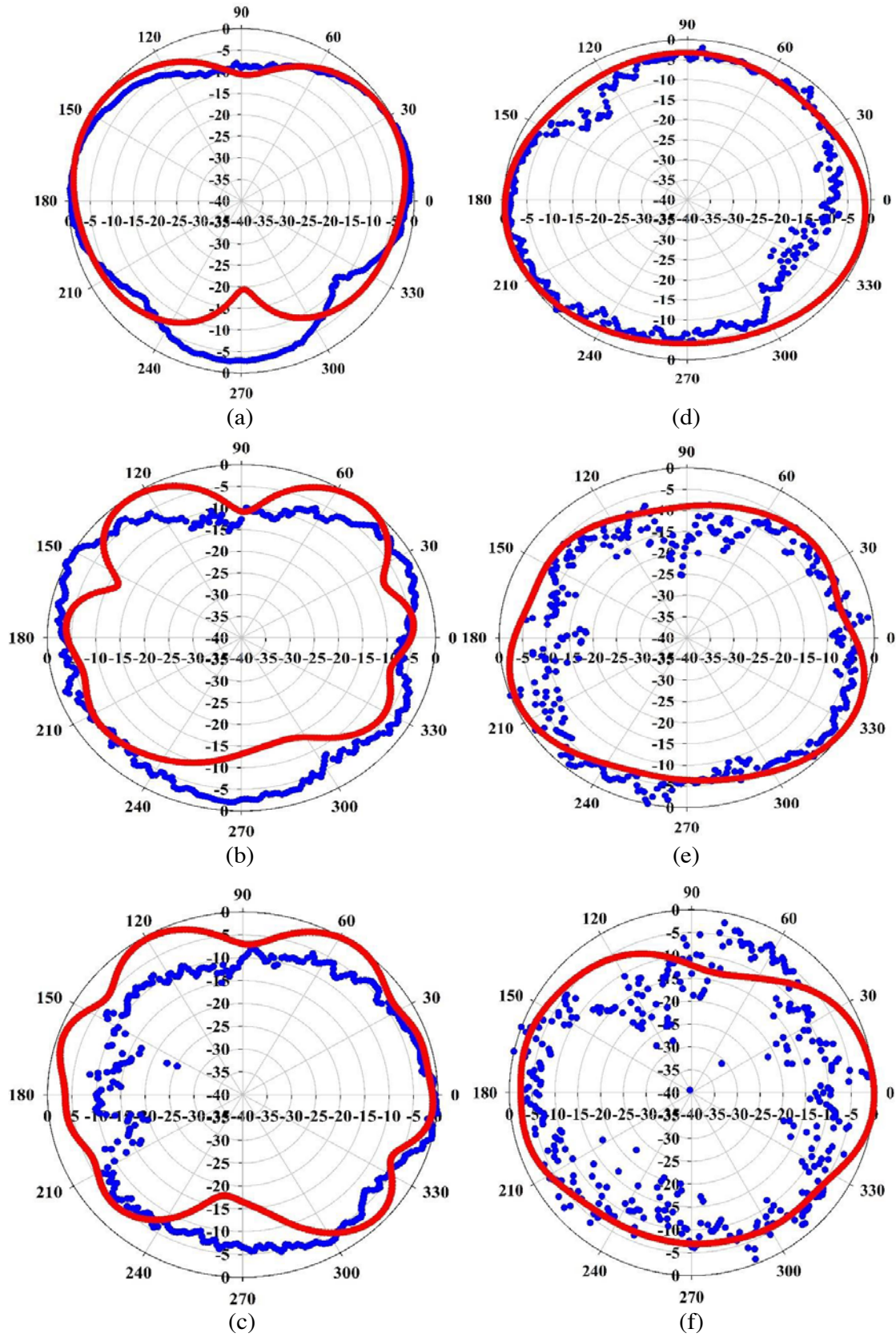
Figure 18. Simulated and measured radiation patterns of antenna 2 at 3.5 GHz, 7.14 GHz, and 9.5 GHz, (a), (b), (c) E-plane, and (d), (e), (f) H-plane.

6. CONCLUSION

This paper reports the experimental investigation of a compact UWB six-element MIMO antenna array. Cross polarization is exploited in order to co-locate diverse antenna elements within a confined space. Based on radiation pattern distinction mechanism, asymmetrical antennas have been used to suppress port-to-port electromagnetic coupling. Experimental results show a high isolation and a good impedance matching characteristic. Also, low envelope correlation coefficients, good radiation characteristics, high efficiency, and gain are verified.

ACKNOWLEDGMENT

CONFLICT OF INTEREST

The authors declare that there is no conflict of interests regarding the publication of this paper.

DATA AVAILABILITY STATEMENT

All data generated during this study are included in this published article.

REFERENCES

1. Khan, S. M., A. Iftikhar, S. M. Asif, A. D. Capobianco, and B. D. Braaten, "A compact four elements UWB MIMO antenna with ON-demand WLAN rejection," *Microw. Opt. Technol. Lett.*, Vol. 58, No. 2, 270–276, 2016.

2. Grau, L., A. Andújar, and J. Anguera, "On the isolation of a MIMO 2 × 2 antenna system using non-resonant elements: 1.71 GHz–2.69 GHz case study," *Microw. Opt. Technol. Lett.*, Vol. 59, No. 9, 2348–2353, 2017.

3. Ibrahim, A. A., J. Machac, and R. M. Shubair, "Compact UWB MIMO antenna with pattern diversity and band rejection characteristics," *Microw. Opt. Technol. Lett.*, Vol. 59, No. 6, 1460–1463, 2017.

4. Wani, Z. and D. Kumar, "A compact 4 × 4 MIMO antenna for UWB applications," *Microw. Opt. Technol. Lett.*, Vol. 58, No. 6, 1433–1437, 2016.

5. Takahashi, K., N. Honma, and K. Murata, "Miniaturized six port MIMO antenna using T-shaped conductor and reactance-loaded notch antenna," *IEICE Communications Express*, Vol. 5, No. 2, 57–62, 2016.

6. Khan, M. U. and M. S. Sharawi, "A 2 × 1 multiband MIMO antenna system consisting of miniaturized patch elements," *Microw. Opt. Technol. Lett.*, Vol. 56, No. 6, 1371–1375, 2014.

7. Xiao, P. E. I., A. L. Borja, and J. R. Kelly, "A technique for MIMO antenna design with flexible element number and pattern diversity," *IEEE Access*, Vol. 7, 86157–86167, 2019.

8. Deng, J. Y., J. Yao, D. Q. Sun, and L. X. Guo, "Ten-element MIMO antenna for 5G terminals," *Microw. Opt. Technol. Lett.*, Vol. 60, No. 12, 3045–3049, 2018.

9. Takahashi, K., N. Honma, K. Murata, and Y. Tsunekawa, "Performance of miniaturized 6-port MIMO antenna using orthogonal polarization," *2014 International Symposium on Antennas and Propagation Conference Proceedings*, Vol. 3, 185–186, 2014.

10. Coetzee, J. C., J. D. Cordwell, E. Underwood, and S. L. Waite, "Single-layer decoupling networks for circulant symmetric arrays," *IETE Tech. Rev. (Institution Electron. Telecommun. Eng. India)*, Vol. 28, No. 3, 232–239, 2011.

11. Al-Hadi, A. A., J. Ilvonen, R. Valkonen, and V. Viikari, "Eight-element antenna array for diversity and MIMO mobile terminal in LTE 3500 MHz band," *Microw. Opt. Technol. Lett.*, Vol. 56, No. 6, 1323–1327, 2014.

12. Mchbal, A., N. Amar Touhami, H. Elftouh, and A. Dkiouak, "Mutual coupling reduction using a protruded ground branch structure in a compact UWB Owl-shaped MIMO antenna," *Int. J. Antennas Propag.*, Vol. 2018, 1–10, 2018.

13. Chen, L., J. Hong, and M. Amin, "A twelve-ports dual-polarized MIMO log-periodic dipole array antenna for UWB applications," *Radioengineering*, 68–73, 2019.

14. Abdullah, M., S. H. Kiani, L. F. Abdulrazak, and A. Iqbal, "High-performance multiple-input multiple-output antenna system for 5G mobile terminals," *Electronics*, Vol. 8, No. 10, 1090, 2019.

15. Satam, V., "Six-element dual polarized high-gain MIMO antenna for multiband applications," *Microw. Opt. Technol. Lett.*, 1–9, March 2019.

16. Amin, F., R. Saleem, T. Shabbir, and S. Rehman, "A compact quad-element UWB-MIMO antenna system with parasitic decoupling mechanism," *Appl. Sci.*, Vol. 9, No. 11, 2371, 2019.

17. Zhai, H., J. Zhang, T. Li, and C. Liang, "A high isolation dual-band MIMO antenna array for multiaccess mobile terminals," *Microw. Opt. Technol. Lett.*, Vol. 57, No. 3, 672–677, 2015.

18. Ahmad, A., "Design and performance analysis of six element MIMO antenna for wireless routers," *2016 19th International Multi-Topic Conference (INMIC)*, 2016.

19. Chen, Z., W. Geyi, M. Zhang, and J. Wang, "A study of antenna system for high order MIMO device," *International Journal of Antennas and Propagation*, Vol. 2016, Article ID 1936797, 2016.